Photochemical Hole-Burning Spectroscopy of Bovine Rhodopsin and Bacteriorhodopsin

Glen R. Loppnow, Richard A. Mathies,*

Department of Chemistry, University of California, Berkeley, California 94720

Thomas R. Middendorf, David S. Gottfried, and Steven G. Boxer*

Department of Chemistry, Stanford University, Stanford, California 94305-5080 *(Received: May 8, 1991; In Final Form: July 26, 1991)*

Photochemical hole burning has been observed at 1.5 K in bacteriorhodopsin (bR) and bovine rhodopsin at wavelengths spanning their lowest energy electronic absorption bands. Hole widths were ~2500 cm^{-1} full width at half-maximum (fwhm) in bacteriorhodopsin and ~2400 cm^{-1} fwhm in rhodopsin. The positions of the hole minima were insensitive to burn wavelength, indicating that minimal site selection occurs at 1.5 K. Simulations of the hole spectra were performed by using the vibronic and line width parameters derived from previous resonance Raman and absorption measurements. Experimental difference absorption spectra were analyzed by fitting them to a sum of the calculated hole spectrum plus the thermalized photoproduct spectrum. These simulated spectra satisfactorily reproduce the burn-wavelength dependence, vibronic features, and widths of the observed holes. The calculations also yield the magnitudes of the homogeneous and inhomogeneous line widths at 1.5 K. In bacteriorhodopsin and rhodopsin, the inhomogeneous line widths deduced from resonance Raman experiments decrease from 1100 and 1800 cm^{-1} fwhm, respectively, at room temperature to 470 and 700 cm^{-1} fwhm at 1.5 K. This observation can be explained by a decrease in the fluctuations in chromophore–protein interactions which leads to a narrowing of the distribution of chromophore transition energies. Extremely broad homogeneous line widths of 1300 cm^{-1} fwhm were determined for rhodopsin and bR at 1.5 K. The absence of a detectable narrow component in spectra burned and probed with 2-cm^{-1} resolution agrees with previous kinetic measurements indicating that rhodopsin and bacteriorhodopsin isomerize on the excited-state surface in ~200–500 fs. The observation that the holes are broad and diffuse is consistent with the ~25-fs optical relaxation times predicted from resonance Raman intensity analyses.

Introduction

Rhodopsins are a class of pigments that mediate light-to-energy and light-to-information transduction. The visual pigment, rhodopsin, is responsible for scotopic or night vision. It is a 41 000 Da intrinsic membrane protein containing an 11-*cis*-retinal prosthetic group bound to lysine-296 via a protonated Schiff base linkage.[1] Bacteriorhodopsin (bR) functions as a light-driven proton pump in the purple membrane of the bacterium *Halobacterium halobium*.[2,3] It is a 26 000 Da intrinsic membrane protein containing an *all-trans*-retinal chromophore attached to lysine-216. The primary photochemical event in both bacteriorhodopsin and rhodopsin is a rapid isomerization of the retinal prosthetic group. Understanding the dynamics and structural changes associated with the excited-state chromophore isomerization in these pigments is a problem of fundamental importance.

Absorption of a photon by the light-adapted form of bacteriorhodopsin is followed by a rapid isomerization of the *all-trans*-retinal chromophore to 13-cis (Figure 1). Analysis of resonance Raman cross sections provided evidence that the homogeneous line width in bacteriorhodopsin is large and accounts for a considerable fraction of the absorption spectral width and diffuseness.[4,5] The large homogeneous line width suggests that the excited-state dynamics may occur on a subpicosecond timescale. Femtosecond absorption studies have shown that at room temperature the chromophore torsionally distorts in the excited state in ~200 fs and then forms the J intermediate in ~500 fs.[6,7] Subsequent relaxation to K occurs in approximately 3 ps.[8-11] Picosecond and low-temperature resonance Raman spectroscopy have demonstrated that the K photoproduct is a 13-cis species.[12-15]

In rhodopsin, the absorption of a photon triggers photoisomerization of the 11-*cis*-retinal chromophore to a twisted all-trans intermediate called bathorhodopsin.[16-20] The photochemical bleaching scheme of rhodopsin is shown in Figure 2. Picosecond absorption[21,22] and Raman[23] studies indicate that the cis–trans isomerization occurs in <6 ps, while modeling of fluorescence quantum yield data[24] suggests a 0.2–0.6-ps time scale for the reaction at room temperature. A recent room-temperature resonance Raman intensity study suggests that excited-state isomerization to a 90° geometry may occur within 200 fs.[25] INDO calculations predict that 2 ps is a reasonable time for the appearance of ground-state bathorhodopsin.[26] These studies indicate

(1) Birge, R. R. *Biochim. Biophys. Acta* **1990**, *1016*, 293.
(2) Mathies, R. A.; Lin, S. W.; Ames, J. B.; Pollard, W. T. *Annu. Rev. Biophys. Chem.* **1991**, *20*, 491.
(3) Khorana, H. G. *J. Biol. Chem.* **1988**, *263*, 7439.
(4) Myers, A. B.; Mathies, R. A. In *Biological Applications of Raman Spectroscopy: Vol. 2-Resonance Raman Spectra of Polyenes and Aromatics*; Spiro, T. G., Ed.; Wiley: New York, 1987; p 1.
(5) Myers, A. B.; Harris, R. A.; Mathies, R. A. *J. Chem. Phys.* **1983**, *79*, 603.
(6) Mathies, R. A.; Brito Cruz, C. H.; Pollard, W. T.; Shank, C. V. *Science* **1988**, *240*, 777.
(7) Dobler, J.; Zinth, W.; Kaiser, W.; Oesterhelt, D. *Chem. Phys. Lett.* **1988**, *144*, 215.
(8) Nuss, M. C.; Zinth, W.; Kaiser, W.; Koelling, E.; Oesterhelt, D. *Chem. Phys. Lett.* **1985**, *117*, 1.
(9) Sharkov, A.; Pakulev, A.; Chekalin, S.; Matveetz, Y. *Biochim. Biophys. Acta* **1985**, *808*, 94.
(10) Polland, H. J.; Franz, M. A.; Zinth, W.; Kaiser, W.; Koelling, E.; Oesterhelt, D. *Biophys. J.* **1986**, *49*, 651.
(11) Petrich, J. W.; Breton, J.; Martin, J. L.; Antonetti, A. *Chem. Phys. Lett.* **1987**, *137*, 369.
(12) Braiman, M.; Mathies, R. *Proc. Natl. Acad. Sci. U.S.A.* **1982**, *79*, 403.
(13) Hsieh, C.-L.; El-Sayed, M.; Nicol, M.; Nagumo, M.; Lee, J.-H. *Photochem. Photobiol.* **1983**, *38*, 83.
(14) Atkinson, G. H.; Brack, T. L.; Blanchard, D.; Rumbles, G. *Chem. Phys.* **1989**, *131*, 1.
(15) Doig, S. J.; Reid, P. J.; Mathies, R. A. *J. Phys. Chem.* **1991**, *95*, 6372.
(16) Yoshizawa, T.; Wald, G. *Nature* **1963**, *197*, 1279.
(17) Oseroff, A. R.; Callender, R. H. *Biochemistry* **1974**, *13*, 4243.
(18) Eyring, G.; Curry, B.; Mathies, R.; Fransen, R.; Palings, I.; Lugtenburg, J. *Biochemistry* **1980**, *19*, 2410.
(19) Eyring, G.; Curry, B.; Broek, A.; Lugtenburg, J.; Mathies, R. *Biochemistry* **1982**, *21*, 384.
(20) Palings, I.; van den Berg, E.; Lugtenberg, J.; Mathies, R. A. *Biochemistry* **1989**, *28*, 1498.
(21) Busch, G. E.; Applebury, M. L.; Lamola, A. A.; Rentzepis, P. M. *Proc. Natl. Acad. Sci. U.S.A.* **1972**, *69*, 2802.
(22) Kandori, H.; Matuoka, S.; Shichida, Y.; Yoshizawa, T. *Photochem. Photobiol.* **1989**, *49*, 181.
(23) Hayward, G.; Carlsen, W.; Siegman, A.; Stryer, L. *Science* **1981**, *211*, 942.
(24) Doukas, A. G.; Junnarkar, M. R.; Alfano, R. R.; Callender, R. H.; Kakitani, T.; Honig, B. *Proc. Natl. Acad. Sci. U.S.A.* **1984**, *81*, 4790.
(25) Loppnow, G. R.; Mathies, R. A. *Biophys. J.* **1988**, *54*, 35.

0022-3654/92/2096-737$03.00/0

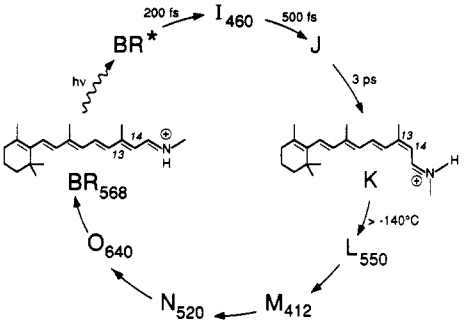

Figure 1. Proton-pumping photocycle of bacteriorhodopsin. Subscripts denote absorption maxima. BR* and I_{460} are excited-state transients. The conversion of K to L is blocked below −140 °C, resulting in a photostationary steady-state composed of bR_{568} and K.

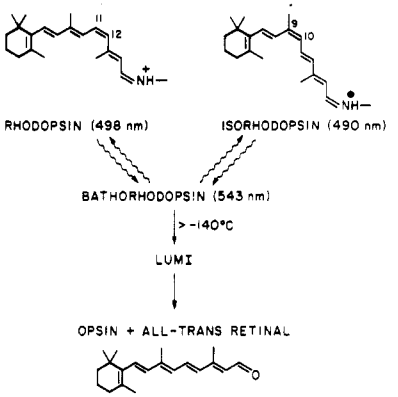

Figure 2. Bleaching scheme of rhodopsin. Numbers in parentheses are absorption maxima at liquid helium temperatures. Conversion of bathorhodopsin to lumirhodopsin is blocked below −140 °C resulting in a photostationary steady-state composed of 11-*cis*-rhodopsin, 9-*cis*-isorhodopsin, and *all-trans*-bathorhodopsin.

that the excited-state isomerization dynamics are extremely fast; hence, the homogeneous component of the overall absorption width is expected to be large.[27]

In both bR and rhodopsin, the initial excited-state photoisomerization reaction proceeds with no apparent change at cryogenic temperatures. However, at such low temperatures subsequent activated reactions are blocked, effectively trapping the primary intermediate. This observation suggests that photochemical hole-burning spectroscopy can be used as a probe of the excited-state dynamics of these pigments at low temperature. A recent photochemical hole-burning study of bacteriorhodopsin and its low-temperature photoproduct estimated that the homogeneous line width is ~400 cm^{-1} half width at half-maximum (hwhm) from the 800 cm^{-1} hwhm hole width; however, contributions to the hole width from vibronic progressions were neglected.[28] Photochemical and nonphotochemical hole-burning spectroscopies have been used previously to characterize the excited states of many chromophore–protein complexes, including bacterial[29-31] and green plant[32-34] photosynthetic reaction centers, antenna complexes,[35-37] phycocyanin,[38] phycoerythrin,[39] and synthetic model complexes.[40] A related site-selection technique, fluorescence line-narrowing spectroscopy, has also been used to study several heme proteins.[41,42]

In this paper, we report photochemical holeburning studies of bovine rhodopsin and bacteriorhodopsin at 1.5 K. Simulations of the hole spectra using line width and vibronic parameters derived from resonance Raman experiments[4,5,25] constitute a stringent check on the magnitude of these parameters and enable us to learn more about the origin and temperature dependence of broadening mechanisms in the absorption spectra of the retinal pigments. The observation of broad holes lacking narrow zero-phonon features[43] in both bacteriorhodopsin and rhodopsin is consistent with the large homogeneous contributions to the absorption bandwidth and fast excited-state dynamics predicted from resonance Raman and transient absorption measurements. In addition, we have found that the inhomogeneous line widths of both pigments are approximately 2.5 times smaller at liquid helium temperature than at room temperature. This result suggests that the distribution of protein–chromophore interactions responsible for wavelength regulation decreases significantly as the temperature is lowered.

Material and Methods

Preparation of Pigments. Bacteriorhodopsin was isolated from an overproducing strain of *H. halobium* (ET1001) using procedures from ref 44. Further purification on sucrose gradients was required to remove carotenoids, which absorb in the 450–600-nm region and overlap with the lowest energy absorption band of bR. The purple membrane fragments were then suspended in a HEPES buffer/glycerol mixture (final concentration 50% glycerol v/v, 12 mM HEPES, 162 mM NaCl, pH 7.0) shortly before the experiment. The final sample concentration was 320 μM, estimated from the extinction coefficient of ϵ_{max} = 62 700 M^{-1} cm^{-1}.

Rhodopsin was isolated from bovine retinas as described previously,[45] concentrated in Amicon membrane cones, and then diluted with glycerol (final concentration 50% glycerol v/v, 50 mM phosphate, <0.5% Ammonyx-LO, <5 mM NH_2OH·HCl, pH 6.8–7.0). The final sample concentration was 400 μM, calculated using an extinction coefficient of ϵ_{max} = 40 000 M^{-1} cm^{-1}.

Isorhodopsin was prepared by regenerating bovine opsin with 9-*cis*-retinal according to established procedures.[45] Briefly, bovine rod outer segments were prepared as above, bleached in the light with hydroxylamine, and washed. The rod outer segments were incubated at room temperature for 1.5 h after adding a 3-fold excess of 9-cis retinal in ~10 μL of ethanol. The resulting isorhodopsin was column purified as described above.

Hole-Burning Spectroscopy. For holeburning experiments on bR, samples were placed in an ice bath and light-adapted by

(26) Birge, R. R.; Hubbard, L. M. *J. Am. Chem. Soc.* **1980**, *102*, 2195.
(27) The hole width corresponding to an excited-state lifetime of 200 fs is 50 cm^{-1}. Pure dephasing, vibrational structure in the electronic transition, and site interconversion (spectral diffusion) on the time scale of the experiment can also contribute to the line width measured by holeburning.
(28) Lee, I. J.; Gillie, J. K.; Johnson, C. K. *Chem. Phys. Lett.* **1989**, *156*, 227.
(29) (a) Boxer, S. G.; Lockhart, D. J.; Middendorf, T. R. *Chem. Phys. Lett.* **1986**, *123*, 476. (b) Boxer, S. G.; Middendorf, T. R.; Lockhart, D. J. *FEBS Lett.* **1986**, *200*, 237.
(30) (a) Meech, S. R.; Hoff, A. J.; Wiersma, D. A. *Chem. Phys. Lett.* **1985**, *121*, 287. (b) Meech, S. R.; Hoff, A. J.; Wiersma, D. A. *Proc. Natl. Acad. Sci. U.S.A.* **1986**, *83*, 9464.
(31) (a) Tang, D.; Jankowiak, R.; Gillie, J. K.; Small, G. J.; Tiede, D. M. *J. Phys. Chem.* **1988**, *92*, 4012. (b) Johnson, S. G.; Tang, D.; Jankowiak, R.; Hayes, J. M.; Small, G. J.; Tiede, D. M. *J. Phys. Chem.* **1989**, *93*, 5953. (c) Tang, D.; Johnson, S. G.; Jankowiak, R.; Hayes, J. M.; Small, G. J.; Tiede, D. M. In *Twenty-Second Jerusalem Symposium: Perspectives in Photosynthesis*; Jortner, J., Pullman, B., Eds.; Kluwer Academic: Dordrecht, 1990; p 99. (d) Johnson, S. G.; Tang, D.; Jankowiak, R.; Hayes, J. M.; Small, G. J.; Tiede, D. M. *J. Phys. Chem.* **1990**, *94*, 5849.
(32) Gillie, J. K.; Fearey, B. L.; Hayes, J. M.; Small, G. J.; Golbeck, J. H. *Chem. Phys. Lett.* **1987**, *134*, 316.
(33) Vink, K. J.; de Boer, S.; Plijter, J. J.; Hoff, A. J.; Wiersma, D. A. *Chem. Phys. Lett.* **1987**, *142*, 433.
(34) Jankowiak, R.; Tang, D.; Small, G. J.; Seibert, M. *J. Phys. Chem.* **1989**, *93*, 1649.
(35) Gillie, J. K.; Hayes, J. M.; Small, G. J.; Golbeck, J. H. *J. Phys. Chem.* **1987**, *91*, 5524.
(36) Gillie, J. K.; Small, G. J.; Golbeck, J. H. *J. Phys. Chem.* **1989**, *93*, 1620.
(37) Johnson, S. G.; Small, G. J. *Chem. Phys. Lett.* **1989**, *155*, 371.
(38) Kohler, W.; Friedrich, J.; Fischer, R.; Scheer, H. *Chem. Phys. Lett.* **1988**, *146*, 280.
(39) Friedrich, J.; Scheer, H.; Zickendraht-Wendelstadt, B.; Haarer, D. *J. Chem. Phys.* **1981**, *74*, 2260.
(40) Boxer, S. G.; Gottfried, D. S.; Lockhart, D. J.; Middendorf, T. R. *J. Chem. Phys.* **1987**, *86*, 2439.
(41) Vanderkooi, J. M.; Moy, V. T.; Maniara, G.; Koloczek, H.; Paul, K.-G. *Biochemistry* **1985**, *24*, 7931.
(42) Koloczek, H.; Fidy, J.; Vanderkooi, J. M. *J. Chem. Phys.* **1987**, *87*, 4388.
(43) Although the coupling in bR and rhodopsin is believed to be vibronic in nature, we use "zero-phonon" because it is the term most commonly used to describe the purely electronic component of an electronic transition.
(44) Braiman, M.; Mathies, R. *Biochemistry* **1980**, *19*, 5421.
(45) Palings, I.; Pardoen, J. A.; van den Berg, E.; Winkel, C.; Lugtenburg, J.; Mathies, R. A. *Biochemistry* **1987**, *26*, 2544.

exposure to room light for 5–15 min. The bR was then loaded into a sample cell composed of two glass slides separated by a 300–400-μm spacer and placed in the dark for 5 min to allow the intermediates in the photocycle to relax to ground-state bR prior to cooling. The samples were cooled to 77 K by immersion into liquid N_2 over a period of 15–30 s, producing clear glasses with minimal cracks. Residual liquid N_2 was then removed under suction, and the ^{4}He immersion dewar (Janis) was immediately filled with liquid He. The samples were protected from extraneous light during the entire cooling process to prevent undesired photochemistry. The temperature was measured (accuracy of ±0.05 K) by monitoring the vapor pressure above the liquid He using a calibrated manometer (Validyne Engineering Corp.). For hole-burning experiments on rhodopsin, the procedure was similar, except the light-adaptation procedure was omitted.

Photochemical hole-burning difference spectra were obtained in the following manner. The transmission was probed using light, chopped at 400 Hz, from a tungsten–halogen bulb that was passed through a $^3/_4$-m double monochromator and detected with either a photomultiplier tube (Hamamatsu R928) operated at low cathode voltage or a Si avalanche photodiode (RCA C30956E). A fraction of the probe beam was split off before the sample to monitor lamp fluctuations, and the signal/reference intensity was measured using lock-in detection. The spectral resolution was ~7 cm^{-1} for low-resolution spectra and ~2 cm^{-1} for high-resolution spectra, and the probe beam power was less than 30 nW/cm^2 at the sample. To ensure that the probe beam was not causing spectral changes, successive transmission scans were subtracted and compared at each burn wavelength prior to irradiation of the sample with the burn laser. No evidence of photochemistry by the probe beam was observed within the detection limits of ~0.2% relative transmission change. Holeburning of the same sample at different wavelengths was performed by moving a tightly fitting, double-sided mask to a fresh (unburned) region of the sample. The transmission spectrum of each of these regions before hole burning at the new wavelength was found to be identical to the spectrum of the sample prior to any holeburning, confirming that only unmasked portions of the sample were exposed to the burn light. Each difference absorption spectrum (containing contributions from the hole and photoproduct spectra) was obtained using the transmission spectrum of the sample before $[T_0(\lambda)]$ and after $[T_b(\lambda)]$ burning:

$$\Delta A(\lambda) = -\log [T_b(\lambda)/T_0(\lambda)] \quad (1)$$

The absorption spectrum of the sample was obtained in a similar fashion using the preburn transmission spectrum and a frozen glycerol/buffer blank as reference. All spectra shown are the average of 2 or 3 scans. Burn wavelengths of 457.9, 476.5, 488.0, and 514.5 nm were produced with an Ar ion laser (Lexel Model 95). Burn wavelengths of 572.0 and 604.4 nm were obtained from an Ar ion laser pumped cw dye laser (Coherent CR-599-21) containing rhodamine 6G; 543.5-nm light was obtained from a green He–Ne laser. Laser line widths were all <1 cm^{-1}. The bR and rhodopsin hole-burning experiments were each repeated on two different sample preparations, and the results were reproducible to within the noise of the measurements.

The dependence of the hole depth on burn time is shown in Figure 3. A plot of the maximum hole depth vs irradiation time (not shown) indicated that the absorption change is linearly dependent on fluence at short (<100 s) burn times. At longer burn times, formation of the photostationary steady state leads to saturation and minimal increase in the hole depth with burn time. To minimize reconversion of the primary photoproducts to the parent species or to secondary photoproducts, and still have sufficient signal-to-noise to detect any significant narrow features in the spectrum, the burn power and time were chosen to produce absorbance changes of 2–5% at the hole minima. For both of the pigments at all wavelengths, this corresponded to irradiation with a 10 μW/cm^2, spatially homogeneous burn beam for approximately 30 s.

Photoproduct Spectra. At low temperature, the thermal decay of the photoproducts in bR and rhodopsin is blocked (Figures 1 and 2). The presence of this trap leads to complications due to the overlap of the photoproduct and hole spectra. This overlap is negligible in most photochemical hole-burning experiments because the photoproduct absorption spectrum is usually far removed in wavelength from the narrow hole spectrum. The overlap is extensive for bR and rhodopsin, however, because the very broad photoproduct spectrum is relatively close in wavelength to the very broad hole spectrum. The experimental difference spectrum $\Delta A(\lambda)$ is thus the sum of the hole spectrum $H(\lambda)$ and the photoproduct absorption spectrum $P(\lambda)$, weighted by the concentrations and extinction coefficients of the ground-state and photoproduct species. The $P(\lambda)$ were obtained experimentally by irradiating bR or rhodopsin with broad-band blue light at 1.5 K until a photostationary state was produced. The compositions of the photostationary-state mixtures are known, allowing us to obtain the absorption spectra of the primary photoproducts by difference methods.[46] Irradiation of bacteriorhodopsin with blue light at 77 K yields a photostationary state composed of bR (72%) and K (28%).[47,48] (The 77 K composition was used for bR because the values at 1.5 K are not known.) At liquid helium temperatures, irradiation of rhodopsin with blue light produces a photostationary state composed of rhodopsin (29%), bathorhodopsin (56%), and isorhodopsin (15%).[16,49] The samples were irradiated at 1.5 K with 100 mW/cm^2 of light with $380 \leq \lambda \leq 480$ nm for bR and $340 \leq \lambda \leq 520$ nm for rhodopsin until no further absorbance change could be detected (typically 30 min). Subtracting 72% of the prebleach bR absorption spectrum from the spectrum after bleaching yields the K spectrum shown in Figure 4A. Subtracting 29% of the prebleach rhodopsin spectrum and 15% of an isorhodopsin spectrum (scaled to an absorbance 1.12 times that of rhodopsin) from the spectrum obtained after irradiation yields the bathorhodopsin spectrum shown in Figure 4B. Scaling of the isorhodopsin spectrum is necessary to account for the difference in extinction coefficients of rhodopsin and isorhodopsin at 1.5 K.[50] The 1.5 K absorption spectrum of isorhodopsin in a 50% (v/v)

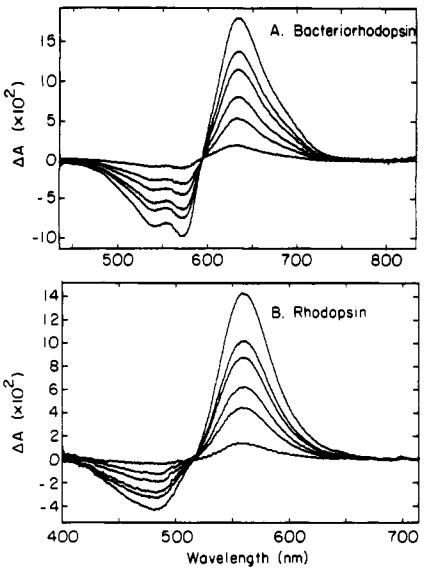

Figure 3. Fluence dependence of the experimental difference spectra in bacteriorhodopsin (A) and rhodopsin (B). Bacteriorhodopsin was irradiated at 572.0 nm and rhodopsin at 514.5 nm with 10 μW/cm^2 for total burn times of 10, 40, 70, 130, 180, and 480 s.

(46) The difference spectra obtained after broad-band irradiation are not to be confused with the difference spectra obtained under low-intensity, narrow-band-excitation "hole-burning" conditions. The broad-band difference spectra were used solely to determine the thermalized 1.5 K absorption spectra of the primary photoproducts, bathorhodopsin and K, whose inhomogeneous site distribution should be randomly populated.

(47) Iwasa, T.; Tokunaga, F.; Yoshizawa, T. *FEBS Lett.* **1979**, *101*, 121.

(48) Hurley, J. B.; Ebrey, T. G. *Biophys. J.* **1978**, *22*, 49.

(49) Yoshizawa, T., personal communication.

(50) Yoshizawa, T. In *Handbook of Sensory Physiology*; Autrum, H., Jung, R., Lowenstein, W. R., MacKay, D. M., Teuber, H. L., Eds.; Springer Verlag: Toyonaka, Osaka, 1972; p 146.

TABLE I: Vibronic Frequencies and Displacements for Rhodopsin and Bacteriorhodopsin[4,5,25]

bacteriorhodopsin			rhodopsin		
mode, cm^{-1}	Δ(1.5 K)[a]	Δ(298 K)	mode, cm^{-1}	Δ(1.5 K)[a]	Δ(298 K)
187	0.77	0.85	98	72 (0.75)[b]	80 (0.82)[b]
266	0.41	0.46	135	207 (1.54)[b]	225 (1.67)[b]
284	0.21	0.23	249	160 (0.63)[b]	174 (0.70)[b]
402	0.26	0.29	262	213 (0.81)[b]	231 (0.88)[b]
452	0.16	0.18	336	117 (0.35)[b]	127 (0.38)[b]
497	0.13	0.14	461	102 (0.22)[b]	111 (0.24)[b]
529	0.11	0.12	809	0.13	0.14
557	0.16	0.18	824	0.15	0.16
830	0.14	0.16	859	0.13	0.14
843	0.12	0.13	970	0.46	0.50
882	0.17	0.19	999	0.13	0.14
959	0.14	0.15	1018	0.29	0.32
1008	0.38	0.42	1189	0.13	0.14
1170	0.38	0.42	1215	0.32	0.35
1201	0.34	0.38	1238	0.37	0.40
1215	0.25	0.28	1268	0.35	0.38
1253	0.15	0.17	1318	0.20	0.22
1273	0.18	0.20	1359	0.18	0.20
1304	0.13	0.14	1389	0.17	0.18
1321	0.15	0.17	1432	0.22	0.24
1333	0.07	0.08	1442	0.23	0.25
1349	0.18	0.20	1549	0.80	0.87
1379	0.08	0.09	1581	0.20	0.22
1448	0.12	0.13	1609	0.27	0.29
1457	0.12	0.13	1659	0.25	0.27
1527	0.63	0.70			
1580	0.14	0.15			
1600	0.12	0.13			
1640	0.19	0.21			

[a] Δ(1.5 K) = $C \times \Delta$(300 K) where C is the linear scaling parameter and is given in Table II. [b] For these lines, the calculation was performed using the linear excited-state model.[25] The excited-state slope $\beta/\hbar$ is given in cm^{-1} and the number in parentheses gives the equivalent harmonic surface displacement calculated using $\Delta\omega = \beta/\hbar$.

glycerol/buffer glass (final concentration 50 mM phosphate, <0.5% Ammonyx-LO, <5 mM NH_2OH·HCl, pH 6.8–7.0) was obtained as described above for rhodopsin.

The absorption spectra of the photoproducts obtained from this decomposition procedure are in agreement with previously published results. The absorption maxima of K (λ_{max} = 625 nm) and bathorhodopsin (λ_{max} = 540 nm) in this study are close to earlier measurements of K (λ_{max} = 628 nm) and bathorhodopsin (λ_{max} = 548 nm) absorption spectra.[16,47] The slight blue shift of rhodopsin's photoproduct spectrum may be due to the different glycerol concentrations and buffer conditions used in the two studies.

Simulation of Absorption Spectra. To simulate the hole-burning spectra we first calculated the absorption spectrum of bR or rhodopsin using the vibronic and line width parameters derived from resonance Raman measurements. The intensities of the resonance Raman lines for a molecule depend on many of the same parameters as the absorption spectrum and provide a sensitive

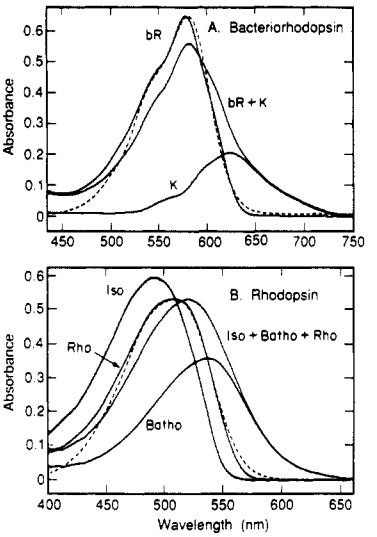

Figure 4. (A) Absorption spectra of bR_{568} and K at 1.5 K for 320 μM bacteriorhodopsin in a 50% v/v glycerol/HEPES buffer glass. Subtraction of 72% of the bR absorption spectrum from the bR + K spectrum yields a pure K spectrum. (B) Absorption spectra of rhodopsin, isorhodopsin, and bathorhodopsin at 1.5 K for 400 μM rhodopsin in a 50% v/v glycerol/phosphate buffer glass. Subtraction of 29% of the rhodopsin absorption spectrum and 15% of the isorhodopsin absorption spectrum from the rho + batho + iso spectrum yields a pure bathorhodopsin spectrum. Dashed lines are the calculated low-temperature absorption spectra of bR_{568} and rhodopsin using the parameters of Tables I and II in eq 1. Discrepancies between the experimental and calculated absorption spectra on the high-energy side are due to scattering in bacteriorhodopsin and a higher electronic state in rhodopsin.

means for determining the relative contributions of homogeneous and inhomogeneous broadening to the spectral band shape.[4] The magnitudes of the homogeneous and inhomogeneous broadening as well as the changes in geometry Δ along specific normal coordinates accompanying electronic excitation have been determined experimentally from self-consistent fits of room-temperature absorption and absolute resonance Raman cross-section excitation profile data for bR and rhodopsin.[4,5,25] The results of these analyses are summarized in Tables I and II. The ground-state absorption spectra of bR and rhodopsin were calculated using a time-dependent wave packet propagation technique that has been described previously.[4,5,25] In the Condon approximation, the absorption cross section is given by:

$$\sigma_A = \frac{4\pi e^2 M^2 E_L}{6\hbar^2 cnW}\sum_i P_i \int_0^\infty \exp-[(E_0 - \langle E_0\rangle)^2/2\Theta^2]\, dE_0 \times \int_{-\infty}^{\infty} \langle i|i(t)\rangle G(t) \exp[i(E_L + \epsilon_i)t/\hbar]\, dt \quad (2)$$

where the summation is over initial vibrational states i, $|i\rangle$ is the initial multimode ground-state vibrational wave function evaluated at time $t = 0$, $|i(t)\rangle = e^{-(iHt/\hbar)}|i\rangle$ is this vibrational wave function propagated on the excited-state surface and H is the excited-state

TABLE II: Line Shape Parameters for Rhodopsin and Bacteriorhodopsin

	homogeneous line width[c] fwhm, cm^{-1}		inhomogeneous line width[d] fwhm, cm^{-1}		Δ scaling parameter (C)	
	1.5 K	298 K	1.5 K	298 K	1.5 K	298 K
bacteriorhodopsin[a]	1300	1300	470	1100	0.90	1.0
rhodopsin[b]	1300	340	700	1800	0.92	1.0

[a] The other parameters in the simulation for bacteriorhodopsin are transition length M = 2.52 Å, refractive index n = 1.33, zero–zero energy E_0 = 17000 cm^{-1}, and homogeneous Lorentzian line width Γ_1 = 50 cm^{-1} from ref 4. The dominant homogeneous broadening was modeled by a 50-cm^{-1} mode with a linear dissociative excited-state potential surface having a slope β of 775 cm^{-1}. This gives rise to a Gaussian homogeneous decay in the time domain $\exp[-(\Gamma_g^2 t^2/\hbar^2)]$ where $\Gamma_g^2 = \{(\omega^2/16) + (\beta^2/4)\}$ and ω is the ground-state frequency in cm^{-1}.[4,5] [b] For the rhodopsin simulation, the parameters are M = 2.079 Å, n = 1.33, and E_0 = 18500 cm^{-1} from ref 25. A Gaussian homogeneous decay function of the form $\exp[-(\Gamma_g^2 t^2/\hbar^2)]$ with Γ_g = 100 cm^{-1} was employed at room temperature and Γ_g = 400 cm^{-1} at 1.5 K. [c] The Gaussian homogeneous line widths Γ_g in eq 2 are related to the frequency domain fwhm values given in this table by Fourier transforming the Gaussian time decays yielding fwhm = $[2(\ln [2(\ln 2)^{1/2}\Gamma_g]/(\pi c\hbar)$. [d] The standard deviations Θ of the Gaussian inhomogeneous line widths in eq 2 are related to the fwhm values given in this table by fwhm = $2(2 \ln 2)^{1/2}\Theta$.

vibrational Hamiltonian, ϵ_i is the initial vibrational energy, E_0 is the variable zero–zero transition energy, and $\langle E_0 \rangle$ its average, E_L is the energy of the incident photon, M is the transition dipole length (in Å), P_i is the fractional population of initial state i, n is the refractive index of the solvent, Θ is the inhomogeneous broadening standard deviation, and $W = \Theta(2\pi)^{1/2}$ is the normalization constant for the inhomogeneous distribution function.

Two different homogeneous contributions to the absorption line shape are indicated in eq 2. First, the explicit Franck–Condon activity is expressed in the $\langle i|i(t)\rangle$ term. At early times $\langle i|i(t)\rangle$ decreases due to the motion of the multimode vibrational wave packet $|i(t)\rangle$ away from the Franck–Condon geometry on the excited-state potential surface. Physically, the multimode overlap $\langle i|i(t)\rangle$ depends on the displacement Δ in equilibrium nuclear coordinates[51] between the ground and excited electronic states along the various normal coordinates; the initial decay of the overlap becomes more rapid as the displacement increases. For most molecules, $\langle i|i(t)\rangle$ is periodic, giving rise to the familiar vibronic structure in the absorption spectrum. In systems like bR and rhodopsin that undergo rapid photochemistry, the long-time recurrences of particularly the low-frequency modes are suppressed and the decay of $\langle i|i(t)\rangle$ is dissipative. For a linear excited-state potential, the decay of $\langle i|i(t)\rangle$ is nearly Gaussian in time.[4,5] The Fourier transform of this time decay leads to a Gaussian homogeneous spectrum in the frequency domain. Details of the methods for the evaluation of $\langle i|i(t)\rangle$ have been described previously.[4] The second homogeneous contribution to the absorption spectrum is $G(t)$, which is a phenomenological homogeneous decay function. Unimolecular stochastic decay processes are often well-described by an exponential time decay, $L(t) = \exp[-(\Gamma_1 t/\hbar)]$, leading to a Lorentzian homogeneous line shape[52] with a fwhm of $\Delta\nu_{homo} = (\Gamma_1/\pi\hbar)$. For rhodopsin and bR, previous resonance Raman measurements indicated that a Gaussian decay, $G(t) = \exp[-(\Gamma_g t/\hbar)^2]$, was necessary in order to account for both the absolute Raman cross sections and the absorption line shape.[4,25] It is important to note that the overall homogeneous line shape contains contributions from $\langle i|i(t)\rangle$, which can be rapid and dissociative for a reactive excited-state potential surface, and from the phenomenological Gaussian decay, which can be attributed to vibronic dephasing, ultrafast electronic relaxation, or modes with large Δ's and low frequencies that are not observed in the resonance Raman spectrum.[25]

The expression for the absorption cross section is a convolution of the single-molecule absorption spectrum, given by the integration over time in eq 2, with an inhomogeneous site distribution function, given by the integration over E_0 in eq 2. The inhomogeneous broadening is modeled by a Gaussian distribution of (0,0) energies with a standard deviation[4] Θ.

Simulation of Hole-Burning Spectra. The single-molecule absorption spectra for bR and rhodopsin were calculated as in eq 2 using the vibronic and line width parameters given in Tables I and II. Simulated hole spectra were generated by "burning" the absorption at each site [discrete (0,0) transition energy]. The effect of burning is to decrease the absorption of the single-molecule spectrum at each site n by depleting the population with that transition energy by an amount proportional to its absorbance at the burn wavelength. The postburn, single-site absorption for site n is then

$$A_{b,n} = A_{o,n} \exp(-\tau k_n) \tag{3}$$

where τ is the burn time, $A_{o,n}$ is the preburn absorption of site n, and k_n is the rate of bleaching of site n. The rate of photobleaching is

$$k_n = \phi \int \sigma_n(\lambda) I_b(\lambda)\, d\lambda \tag{4}$$

where ϕ is the isomerization quantum yield, $\sigma_n(\lambda)$ is the magnitude

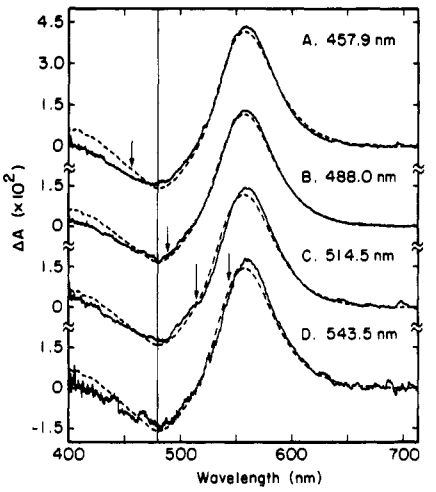

Figure 5. Experimental (—) and calculated (---) difference spectra for rhodopsin. The spectra were obtained by irradiating the sample with 10 μW/cm^2 of (A) 457.9, (B) 488.0, (C) 514.5, and (D) 543.5-nm light for 30 s at the positions indicated by the vertical arrows. Simulations of the difference spectra were performed as described in the text using the parameters in Tables I and II.

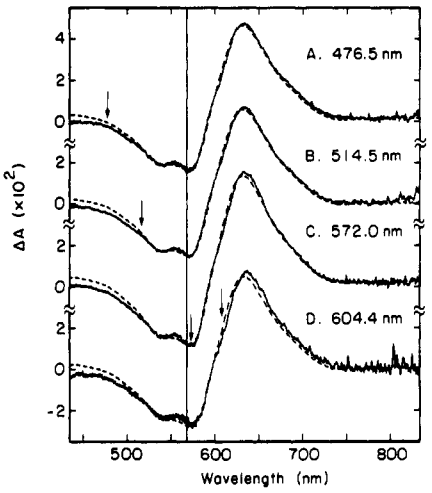

Figure 6. Experimental (—) and calculated (---) difference spectra for bacteriorhodopsin. The spectra were obtained by irradiating the sample with 10 μW/cm^2 of (A) 476.5, (B) 514.5, (C) 572.0, and (D) 604.4-nm light for 30 s at the positions indicated by the vertical arrows. Simulations of the difference spectra were performed as described in the text using the parameters in Tables I and II.

of the absorption cross section, and $I_b(\lambda)$ is the intensity of the burn beam. The calculated hole spectrum $H_{calc}(\lambda)$ is then the difference between the calculated burned and unburned absorption spectra. This approach to simulating the hole spectra is similar to the method described by Friedrich et al.[53] The experimental difference absorption spectrum $\Delta A(\lambda)$ was fit to a sum of the calculated hole spectrum $H_{calc}(\lambda)$ and the experimental photoproduct spectrum $P(\lambda)$ using a linear least-squares fit of the equation

$$\Delta A(\lambda) = b[aP(\lambda) + H_{calc}(\lambda)] \tag{5}$$

where a and b are the fitting parameters. This model assumes that the only species present in the difference spectra are the residual parent and primary photoproduct. The presence of an isoabsorptive point in the difference spectra of bR and rhodopsin, as shown in Figure 3, is consistent with the presence of only two interconvertible species. In addition, for the small burns used in these experiments, in which only 2–5% of the molecules are photoaltered, the fraction of photoproduct molecules that reisomerizes is only 0.04–0.3%. We note that the above analysis is rigorously correct only if the line shapes of the photoproducts

(51) Δ is the displacement in dimensionless normal coordinates; the transformation to Cartesian coordinates x is $\Delta = x(\mu\omega/\hbar)^{1/2}$, where μ is the reduced mass of the oscillator and ω its frequency.

(52) $\Gamma_1/\hbar$ is equivalent to $1/T_2$ in the exponential decay $L(t) = \exp[-t/T_2]$. The fwhm $\Gamma_1/\pi\hbar$ corresponds to the familiar relation $\Delta\nu_{homo} = 1/\pi T_2$.

(53) Friedrich, J.; Swalen, J. D.; Haarer, D. *J. Chem. Phys.* **1980**, *73*, 705.

produced by broad-band and narrow-band irradiation of the parent compounds are identical[54] and if the photochemical quantum yield is wavelength-independent.

Results

The experimental hole spectra for rhodopsin and bacteriorhodopsin are shown in Figures 5 and 6 for a variety of burn wavelengths spanning their absorption bands. Hole widths are ~2400 cm^{-1} full-width at half-maximum (FWHM) in rhodopsin and ~2500 cm^{-1} FWHM in bacteriorhodopsin. The positions of the hole minima in rhodopsin change by only ~270 cm^{-1} for a range of burn wavelengths from 457.9 to 543.5 nm (a range of 3440 cm^{-1}). In bacteriorhodopsin, the hole position changes by ~120 cm^{-1} for burn wavelengths from 476.5 to 604.4 nm (a range of 4441 cm^{-1}). The difference spectra of bacteriorhodopsin also exhibit partially resolved vibronic structure with an approximately 1500-cm^{-1} spacing between features, corresponding to the 1527-cm^{-1} C=C ethylenic stretch. No vibronic features are evident in the hole spectra of rhodopsin, although the Raman cross section of the ethylenic stretch at 1549 cm^{-1} in rhodopsin is similar to that of the 1527-cm^{-1} band in bR.

Initial calculations of the absorption and hole spectra using the room-temperature resonance Raman parameters resulted in simulated difference spectra which did not reproduce the experimental spectra. The simulated hole positions were too dependent on the burn wavelength, and the calculated hole spectra for rhodopsin exhibited vibronic structure which was not observed in the experimental spectra. Because of these discrepancies, it was necessary to adjust the overall scaling of the Δ's and the line-width parameters Γ and Θ to simultaneously reproduce the experimental 1.5 K absorption and difference spectra. (The vibrational frequencies and the relative magnitudes of the Δ's were not changed from their room-temperature values.) These three parameters can be optimized separately because they affect the absorption and hole spectra differently. The Δ scaling factor C affects the width of the absorption spectrum, Γ contributes to the diffuseness of the hole and absorption spectra, and Θ determines the sensitivity of the hole spectrum to burn wavelength and contributes to the diffuseness of the absorption spectrum. For each set of Γ, Θ, and C values, the absorption spectrum and the hole spectra at all four experimental burn wavelengths were calculated. The calculated hole spectra were combined with the experimental photoproduct spectrum and fit to the experimental difference spectra. The χ^2 from the fits to the difference spectra were added to the scaled χ^2 for the fit to the parent absorption spectrum to give a total χ^2. Iteration of this process for a wide range of Γ, Θ, and C values yielded optimized parameters consistent with all experimental hole and absorption spectra. χ^2 generally increased by ~10% for changes of ~250–300 cm^{-1} in the fwhm of the homogeneous and inhomogeneous line widths. The quality of the fits is significantly decreased for changes of 150–200 cm^{-1} in these parameters. We therefore assign them an error of ±200 cm^{-1}. The simulated absorption and difference absorption spectra shown in Figures 4–6 fit the experimental data quite well. The calculated absorption spectra correctly reproduce the vibronic features and band shape in bacteriorhodopsin and rhodopsin. The hole spectra simulations also correctly reproduce the vibronic features in bacteriorhodopsin, the absence of vibronic features in rhodopsin, and the weak burn-wavelength dependence of the hole spectra in both pigments. The largest errors in the fits are on the short-wavelength edges of all the spectra. These discrepancies are likely due to spectral overlap with higher lying excited states which have not been considered in the simulations. Wavelength-dependent scattering may also contribute to the increased absorption on the blue side

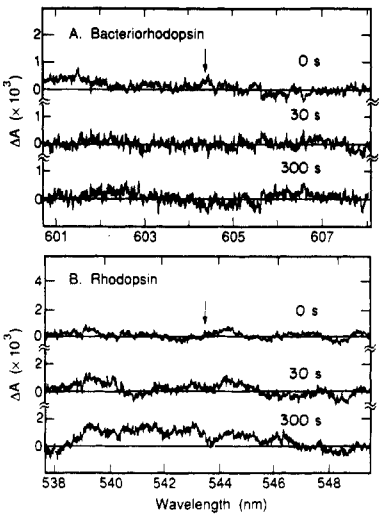

Figure 7. High-resolution difference absorption spectra of (A) bacteriorhodopsin and (B) rhodopsin. Bacteriorhodopsin was irradiated with 10 $\mu W/cm^2$ at 604.4 nm and rhodopsin was irradiated with 10 $\mu W/cm^2$ at 543.5 nm. The three curves show ΔA after burning for 0, 30, and 300 s. A linear background has been subtracted from each spectrum to facilitate display and the arrows indicate the burn wavelengths.

of the experimental absorption spectra.

The final low-temperature parameters are compared with the room-temperature values in Table II. To account for the burn-wavelength independence of the holes, the inhomogeneous line width in bacteriorhodopsin was decreased from 1100 cm^{-1} at 298 K to 470 cm^{-1} fwhm at 1.5 K. In rhodopsin the inhomogeneous width was decreased from 1800 cm^{-1} at 298 K to 700 cm^{-1} at 1.5 K. It was necessary to increase the homogeneous line width of rhodopsin from 340 cm^{-1} at 298 K to 1300 cm^{-1} fwhm at 1.5 K. At room temperature, thermal excitation of the low-frequency modes contributes members to the ensemble average that exhibit faster decay of their torsional $\langle i|i(t)\rangle$. If this were a dominant contribution to the homogeneous line shape, then cooling the sample should result in increased resolution and a narrower hole because the torsional degrees of freedom are no longer thermally excited. It is striking that the hole shape in rhodopsin does not sharpen at low temperature, and this is mirrored by the large homogeneous line width necessary to model the 1.5 K data (Table II). One possibility is that the dominant homogeneous decay mechanism changes between room temperature and 1.5 K. This explanation is inconsistent with the temperature independence of the primary photochemistry. A second more likely possibility is that the 1300-cm^{-1} homogeneous Gaussian decay process is active at both temperatures and the effect of the thermally excited low frequency modes does not in fact dominate the room-temperature homogeneous line shape. This suggests that the previous analysis of the resonance Raman intensities[25] should be redone using the more physical model for the Gaussian decay that is introduced below. It is also possible that the homogeneous line width deduced from our analysis may be affected if the Δ and ω for the coupled modes change appreciably between room temperature and 1.5 K, since room-temperature Δ's and ω's were used in the analysis of the low-temperature absorption and hole-burning spectra. No analogous increase in Γ was required to fit the bR data. Finally, the Δ scaling factor C was decreased by ~10% from room to low temperature for both pigments. This is within the experimental error reported for the room-temperature measurement and is not considered to be physically significant.[4,5,25]

Narrow zero-phonon holes with widths in the range 0.001 to 1.0 cm^{-1} and which are centered at the burn wavelength have been observed at low temperature for a large number of molecules in crystalline, polymer, and protein matrices (see refs 55–57 for

(54) There is evidence from experiments on mixed crystals that photoproduct ("antihole") spectra can be significantly narrower than equilibrium ground-state spectra. [Olson, R. W.; Lee, H. W. H.; Patterson, F. G.; Fayer, M. D.; Shelby, R. M.; Burum, D. P.; Macfarlane, R. M. *J. Chem. Phys.* **1982**, *77*, 2283]. In the present experiments, such site selection was not observed. The broad-band bleach spectra and the difference spectra obtained under hole-burning conditions were found to be nearly indistinguishable in the regions of the photoproduct absorptions, which was taken as justification for the decomposition method described by eq 5.

(55) Small, G. J. In *Spectroscopy and Excitation Dynamics of Condensed Molecular Systems*; Agranovich, V. M., Hochstrasser, R. M., Eds.; North Holland: Amsterdam, Netherlands, 1983; p 515.

(56) Friedrich, J.; Haarer, D. *Angew. Chem., Int. Ed. Engl.* **1984**, *23*, 113.

reviews). We probed for narrow holes in bacteriorhodopsin and rhodopsin by carefully measuring difference absorption spectra in a 100-cm^{-1} region on either side of the burn wavelength with 2-cm^{-1} spectral resolution. Although this resolution would be too poor for the accurate measurement of hole widths in most systems, it does not pose a problem in these experiments. Since the excited-state lifetimes in bR and rhodopsin are both $\leq$6 ps, the minimum hole width permitted by the uncertainty principle is approximately 2 cm^{-1} or greater. The results are shown in Figure 7 for bR burned at 604.4 nm and for rhodopsin burned at 543.5 nm. No narrow holes were observed in the difference spectra of either pigment within the detection limits of 0.2% relative absorbance change. Burning at longer wavelengths in bR or rhodopsin would be a useful experiment; however, this is not possible because of complications resulting from the large spectral contributions from photoproducts.[58]

Discussion

Excited-State Dynamics in Rhodopsins. The observation of very broad photochemical holes lacking narrow features at the burn wavelength in bacteriorhodopsin and rhodopsin is consistent with previous resonance Raman intensity and transient absorption measurements which indicate that there is an extremely rapid photoisomerization in these pigments. Analysis of the resonance Raman intensities of bacteriorhodopsin demonstrated that the large absorption band width and diffuseness arise from progressions in many vibrational modes, each of which is broadened by a $\sim$1300 cm^{-1} FWHM homogeneous line width.[4] In bacteriorhodopsin, the large homogeneous line width is presumed to arise from geometric distortions along dissociative torsional coordinates and concomitant electronic structure alterations. Consistent with the resonance Raman intensity analysis, femtosecond absorption experiments on bacteriorhodopsin provided evidence for torsional departure from the Franck–Condon region on a 200-fs time scale.[6] These torsional degrees of freedom were directly observed in the resonance Raman spectrum of rhodopsin, and analysis of their intensities suggested that torsional departure from the Franck–Condon region occurs in tens of femtoseconds.[25] Thus far, no direct, time-resolved measurement of the cis–trans isomerization in rhodopsin has been reported. The large homogeneous line widths for rhodopsin and bacteriorhodopsin derived from the resonance Raman intensity analysis coupled with strong Franck–Condon activity in many modes suggest that photochemical holes in these molecules should be very broad. Our observation and satisfactory modeling of the 2400–2500-cm^{-1} fwhm hole widths in bacteriorhodopsin and rhodopsin confirms the line width parameters indicated in the resonance Raman intensity and femtosecond absorption studies and are consistent with a 200–500-fs time scale for the isomerization of the retinal chromophore. We emphasize that the overall hole width is not simply related to the isomerization time for bR or rhodopsin. It is the absence of detectable narrow zero-phonon holes in the difference spectra that is inconsistent with electronic lifetimes that are longer than $\sim$200–500 fs (vide infra).

Zero-Phonon Hole Intensity. For a two-level system, the homogeneous line width Γ of an electronic transition is related to the total dephasing time T_2 of the excited-state level[59] as:

$$\Gamma\ (cm^{-1}) = 1/(\pi c T_2) = [1/(2\pi c T_1)] + [1/(\pi c T_2^*)] \quad (6)$$

where T_1 is the excited state lifetime, T_2^* is the pure dephasing time, c is the speed of light, and Γ is the homogeneous line width (fwhm) in cm^{-1}. In the limit that the zero-phonon hole width is negligible compared to the inhomogeneous width, the hole width is simply twice the homogeneous line width.[60] Extremely broad hole widths may thus result from ultrafast excited-state dynamics. For systems like bR and rhodopsin, the two-level system approximation is not valid because the vibronic progressions in the many modes which are coupled to the electronic transition will also contribute to the hole line shape. In this case the single-molecule absorption spectrum, and by extension the hole width, is not simply related to the total dephasing rate of the excited state, but rather is determined by the contour of Franck–Condon profiles for all of the coupled phonon and vibrational modes, each of which is broadened by an amount proportional to its total dephasing rate. Normally, both a narrow zero-phonon hole and a broader phonon sideband are observed in hole-burning spectra; the observation of a single broad feature in the rhodopsin and bacteriorhodopsin hole burning precludes such an obvious assignment.

Below we present a calculation of the expected relative integrated intensity of the zero-phonon component of the hole and the component due to vibronic progressions using the known vibronic displacements for these molecules (Table I). Our goal is to explore whether there might be a narrow zero-phonon hole in rhodopsin or bR whose amplitude is too small to be observed.

The factors which determine the relative areas under the zero-phonon line, I_z, and the phonon sideband, I_p, in absorption spectra have been quantitatively described in the context of a simple configuration coordinate model.[61,62] If the ground and excited-state surfaces are considered harmonic, and Duschinsky rotations and frequency changes are neglected, then the intensity of each vibronic band in a molecule can be expressed as the appropriate product of the individual Franck–Condon factors for all of the modes in the molecule. The 0–0 Franck–Condon factor for each mode i is given by exp $(-S_i)$ where

$$S_i = \tfrac{1}{2}\Delta_i^2 \quad (7)$$

where S_i is the Huang–Rhys factor[61] and Δ_i was defined previously. The intensity of the pure 0–0 transitions, in which there is no vibrational or phonon excitation in any mode accompanying electronic excitation, is thus $\exp(-S_{total})$ where $S_{total} = \sum_i S_i$. At zero temperature, the Debye–Waller factor α is given by[62,63]

$$\alpha = I_z/(I_z + I_p) = \exp(-S_{total}) \quad (8)$$

In the context of holeburning, model calculations have predicted that the zero-phonon hole and phonon sideband hole intensities are related by a "hole-burning" Debye–Waller factor of approximately $\exp(-2S_{total})$.[64] For bR, the total S calculated from eq 7 and the Δ's in Table I is 1.06, implying that the zero-phonon hole will comprise approximately 12% of the total hole intensity. If the electronic T_2 for the excited state of bR were 500 fs or longer, then the *amplitude* of the zero-phonon hole (with width $\leq$20 cm^{-1} fwhm) would be *larger* than that of the $\sim$2500 cm^{-1} fwhm sideband hole. The much stronger coupling in rhodopsin (S_{total} = 2.96) leads to a predicted zero-phonon hole with 0.2% of the total hole intensity. The amplitude of a 20-cm^{-1} zero-phonon hole in this case would be approximately 20% of the maximum amplitude of the vibronic sideband hole, clearly observable given the signal-to-noise ratio of our data. We conclude from this analysis that the homogeneous line widths in these systems must be considerably greater than 20 cm^{-1}. The absence of any observable narrow feature at the burn wavelength in any of the

(57) Völker, S. *Annu. Rev. Phys. Chem.* **1989**, *40*, 499.

(58) In photochemical holeburning studies of the primary electron donor in photosynthetic reaction centers, it has been empirically and theoretically demonstrated that the amplitude of the zero-phonon hole relative to the phonon sideband hole increases as the burn wavelength is tuned to the red edge of the absorption spectrum (see refs 64 and 75). In proportion to the absorption spectra, our red-most burn wavelengths in bR and rhodopsin are as far on the low-energy side of the band as the burn wavelengths which yielded narrow zero-phonon holes in reaction centers.

(59) Sargent, M., III; Scully, M. O.; Lamb, W. E., Jr. *Laser Physics*; Addison-Wesley: Reading, MA, 1974.

(60) de Vries, H.; Wiersma, D. A. *J. Chem. Phys.* **1980**, *72*, 1851.

(61) Huang, K.; Rhys, A. *Proc. R. Soc.* **1950**, *A204*, 406.

(62) Pryce, M. H. L. In *Phonons*; Stevenson, R. W. H., Ed.; Plenum: New York, 1966.

(63) Fitchen, D. B.; Silsbee, R. H.; Fulton, T. A.; Wolf, E. L. *Phys. Rev. Lett.* **1963**, *11*, 275.

(64) (a) Hayes, J. M.; Small, G. J. *J. Phys. Chem.* **1986**, *90*, 4928. (b) Hayes, J. M.; Gillie, J. K.; Tang, D.; Small, G. J. *Biochim. Biophys. Acta* **1988**, *932*, 287. This analysis indicated that the relative magnitude of the zero-phonon hole is $\exp(-2S)$ only when the burn wavelength is in the vicinity of the maximum of the inhomogeneous distribution function. The zero-phonon hole increases in intensity relative to the broad sideband hole as the burn wavelength is shifted to the red. In the present experiments, the burn wavelengths bracketed the peak of the inhomogeneous distribution for bR and rhodopsin, so the $\exp(-2S)$ approximation is valid.

holeburning spectra strongly supports the extremely rapid optical relaxation times predicted for bR and rhodopsin from the analysis of resonance Raman intensities. Based on these two independent measurements, we conclude that the possibility of narrow homogeneous line widths in these systems can be confidently rejected.

Several factors may contribute to the breadth of the observed holes and the inability to observe zero-phonon holes. First, there may be very low frequency, strongly coupled modes that were not observed in the resonance Raman experiments. The effect of such modes would be to decrease the expected zero-phonon hole intensity. However, for the signal-to-noise ratio of the holeburning data in Figures 5–7, the total Huang–Rhys factors in bR and rhodopsin would have to be greater than about 4.2 in order for a 20-cm^{-1} fwhm zero-phonon hole to remain unobserved.[65] Furthermore, if such low-frequency modes were dominant they would result in a strongly temperature-dependent line width with a much reduced value at 1.5 K. If anything, the opposite behavior is observed. Second, site interconversion occurring on the time scale of hole-burning experiments (many minutes) also contributes to the homogeneous line width measured in holeburning experiments;[66] however, these broadening effects due to "spectral diffusion" are typically fractions of a wavenumber at 1.5 K, an amount which is negligible compared to the widths of the holes observed in the present study. In addition, the fact that narrow (less than 1 cm^{-1} fwhm) zero-phonon lines are observed in many protein–chromophore complexes[38-40] suggests that site interconversion rates are not anomalously fast in protein matrices. It is unlikely then that the extremely broad holes observed in bR and rhodopsin can be attributed to extremely rapid site interconversion rates. Finally, the large homogeneous line widths in bR and rhodopsin should further obscure possible structure in the hole spectra. The calculated difference spectra shown in Figures 5 and 6 represent the synthesis of all of these effects.

Physical Interpretation of the Homogeneous Width. For a complete understanding of the photophysical dynamics of rhodopsins, we must elucidate the physical origin of the phenomenological Gaussian decay process $G(t)$. One possibility is that this decay is due to a number of low-frequency torsional modes that are highly displaced and whose ground-state vibrational frequencies are too low to be observed in the Raman experiment. This explanation is appealing for these vibrationally complex systems, but it suffers from one critical flaw. As illustrated for rhodopsin, such low-frequency modes must be thermally excited at room temperature and their contribution to the absorption line shape must decrease dramatically as the temperature is reduced. In contrast to this prediction, the *overall* homogeneous line shapes in rhodopsin and bR are nearly temperature independent, and no significant sharpening occurs at 1.5 K. Thus, the broadening must come from some other temperature-independent mechanism. This broadening cannot arise from vibronic activity in displaced high-frequency modes because this effect has already been explicitly accounted for. An appealing explanation is that the rapidly decaying $G(t)$ is due to a change in electronic character as the chromophore undergoes torsional deformation. States with A_g and B_u character are known to lie very close to one another in rhodopsins,[67] and calculations by Dormans et al.[68] for simple polyene protonated Schiff bases have indicated that torsional distorsion can dramatically alter the mixing between these electronic configurations. The rapid phenomenological Gaussian decay of 1300 cm^{-1} in both rhodopsin and bR could correspond to a rapid mixing of "A_g character" into the initial "B_u" state as the chromophore torsionally distorts. The Gaussian decay arises because the initial torsional displacement depends quadratically on time.[4,5] In this case, the Condon approximation used to derive eq 2 is no longer valid, and the transition moment M cannot be removed from the wavepacket overlap integral. Rather, this integral should be written $\langle i|M(Q)\exp[-iHt/\hbar]M(Q)|i\rangle$ where the coordinate dependence of the transition moment is now explicit. In our analysis, the Gaussian $G(t)$ is simply a convenient way of parameterizing the role of $M(Q)$. The large coordinate dependence of the electronic transition moment is another way to describe the vibronic dephasing of the wave packet discussed by Mathies et al. as one approaches a Landau–Zener electronic surface crossing.[6] This picture is analogous to that recently used to explain the Gaussian homogeneous line shapes found in pericyclic photochemical rearrangements.[69] A strong coordinate dependence to the transition moment may also be revealed by looking for torsional modes which exhibit B-term enhancement.[4]

Temperature Dependence of Inhomogeneous Broadening. By comparing the previously measured room-temperature vibronic and line shape parameters for rhodopsin and bacteriorhodopsin with the results of the present 1.5 K hole-burning study, we have quantitatively evaluated the temperature dependence of these parameters. For both pigments, the inhomogeneous line width at low temperature is smaller than at room temperature (Table II). A model of inhomogeneous broadening in visual pigments attributes the differences in site energy to fluctuations in the protein–chromophore interactions responsible for wavelength regulation.[70] There is a significant temperature dependence to the spectral sensitivity curves of the toad rod,[71] suggesting that these fluctuations are temperature-dependent. If the width of the inhomogeneous distribution is determined by the extent of these fluctuations, then it should be temperature dependent as well. Spectroscopic data on a wide variety of compounds[72] also suggests that the inhomogeneous line width is determined by the distribution of available (i.e. thermally accessible) guest–host geometries. The geometries which can be sampled depend on the motion of the guest and host. When the temperature is reduced the distribution of geometries is narrowed and the inhomogeneous width should be reduced, as observed. Interpreting the temperature dependence of the inhomogeneous line width in terms of dynamics may be complicated by two factors. First, the relevant timescale for resonance Raman scattering is much faster than that for hole burning. Therefore, those components of spectral diffusion which are slow relative to T_2 may appear as inhomogeneous broadening in a resonance Raman experiment and as homogeneous broadening in a hole-burning experiment. Second, the *rate* of spectral diffusion may be temperature dependent. Thus motions which contribute to the inhomogeneous line width measured in a low-temperature resonance Raman measurement may appear as homogeneous broadening in the same measurement at high temperature. Resonance Raman cross-section measurements on bR and rhodopsin at low temperature may provide further information on these questions. However, these complications do not affect the basic conclusion that the inhomogeneous line widths of bR and rhodopsin are much larger at room temperature than at low temperature.

Relationship to Previous Work. While this work was in progress, an independent study of photochemical hole burning in bacteriorhodopsin was reported by Lee et al.[28] Their results are both quantitatively and qualitatively different from those presented here. The hole widths in the earlier study were ~1600 cm^{-1} fwhm, but no vibronic features were observed. Also, the expected photoproduct absorption[47] was absent in their difference spectra. Figure 3 in the present work illustrates that burning with 110 mW/cm^2 for 5 min (the fluence used in ref 28) should produce a photostationary steady state with a prominent photoproduct absorption. Finally, Lee et al. conclude from a line-shape analysis of the bacteriorhodopsin hole at one burn wavelength that the inhomogeneous line width at low temperature is similar to that at room temperature. We have shown that there is a significant narrowing

(65) The limits on the amount of coupling in low-frequency modes has also been discussed extensively in refs 5 and 25.

(66) Berg, M.; Walsh, C. A.; Narasimhan, L. R.; Littau, K. A.; Fayer, M. D. *Chem. Phys. Lett.* **1987**, *139*, 66; *J. Chem. Phys.* **1988**, *88*, 1564.

(67) Birge, R. R.; Zhang, C.-F. *J. Chem. Phys.* **1990**, *92*, 7178.

(68) Dormans, G. J. M.; Groenenboom, G. C.; van Dorst, W. C. A.; Buck, H. M. *J. Am. Chem. Soc.* **1988**, *110*, 1406.

(69) Trulson, M. O.; Dollinger, G. D.; Mathies, R. A. *J. Chem. Phys.* **1989**, *90*, 4274.

(70) Loppnow, G. R. Ph.D. Thesis, UC Berkeley, 1990.

(71) Lamb, T. D. *J. Physiol.* **1984**, *346*, 557.

(72) Thijssen, H. P. H.; Dicker, A. I. M.; Völker, S. *Chem. Phys. Lett.* **1982**, *92*, 7.

of the inhomogeneous line width as the temperature is lowered. The 5 order of magnitude greater burn fluences used by Lee et al. may account for these differences.

Comparison with Photochemical Holes in Photosynthetic Reaction Centers. There are many similarities between the results reported here and previous hole-burning experiments on photosynthetic reaction centers (RCs).[29-31] In the latter experiments, narrow band width excitation in the lowest energy absorption band of the primary electron donor P at 1.5 K in RCs from the bacteria *Rb. sphaeroides* and *Rps. viridis* resulted in the hole spectra with widths of 400–500 cm^{-1}, or approximately 80–100% of the absorption bandwidth. No narrow features at the burn wavelength were observed in the initial experiments. As in the present experiments, the broad holes were only weakly dependent on burn wavelength. Two different initial interpretations of these results were presented.[29] It was noted that if the hole width were primarily determined by lifetime broadening, then a decay time of ~20–200 fs for the initially excited state is predicted.[29,30] An alternative proposal, that the zero-phonon hole is suppressed and the hole is broad and diffuse due to changes in the equilibrium nuclear coordinates along one or more modes coupled to the electronic transition, was also considered.[29] Subsequent theoretical models related to the second proposal above considered the effects of strong coupling of low-frequency vibrations or phonons to the electronic excitation of P.[64,73] Recently, narrow zero-phonon holes of extremely small relative amplitude have been observed when the burn wavelength is tuned to the low-energy edge of the absorption spectrum of the primary donor.[31] The width of these holes (~10 cm^{-1} fwhm) is, within the signal-to-noise, equal to the width expected for an electronic lifetime of ~1 ps, the low-temperature time constant for the initial electron-transfer reaction measured by transient absorption.[74] In recent experiments these results have been confirmed.[75] It was also found that the zero-phonon hole width decreases to approximately 1 cm^{-1} fwhm in mutant reaction centers in which the initial electron-transfer rate slows to approximately 10 ps.[75] Taken together, these results strongly suggest that the zero-phonon hole widths are determined by the excited-state lifetime in these RCs. In addition, the electronic dynamics can be separated from the vibrational dynamics in the RC by observation of the zero-phonon hole. In bR and rhodopsin the relative contributions of these two components of the dynamics to the homogeneous line width cannot be separated because the zero-phonon hole is so broad that it is not experimentally resolved from the vibronic sideband component of the hole.

There are many interesting parallels between the primary photochemistry in reaction centers and the systems studied here. The vibronic coupling is unusually strong in these systems. Analysis of the absorption and hole line shapes in the RC suggested that the total Huang–Rhys factor for the P absorption band is large, ~3.7,[31,75] and similar in magnitude to the coupling in rhodopsin, where the total $S = 2.96$. The observation of intense zero-phonon holes in a variety of large aromatic molecules indicates that such strong coupling is not present in most systems. The physical origin of the strong coupling in rhodopsin and RCs is still uncertain. The large nuclear displacements upon photoexcitation arise from a dramatic redistribution of electrons in the excited state which is correlated in these systems with a large change in the polarity between the ground and excited states. Both retinal[67,76] and the primary donor in RCs[77-79] have large changes in permanent dipole moment between their ground and lowest excited electronic singlet state. We are presently exploring the quantitative relationship between difference dipole moments and hole widths in synthetic model systems using a combination of hole-burning and Stark spectroscopies.[80] Another interesting possibility is that the strong coupling has functional consequences in these systems. In rhodopsin, resonance Raman studies[25] suggest that some of the coordinate displacements that occur upon electronic excitation are along the same torsional degrees of freedom involved in isomerization. In the reaction center, the analogous question is whether the modes that are coupled to the absorption transition serve as promoting or accepting modes for the initial electron transfer. In other words, is the state that is formed upon absorption of a photon distorted along the reaction coordinate for electron transfer? Currently there is little mode-specific information available on the P band;[75] however, a recurring consideration is the role of strongly coupled low-frequency modes.[29,31,64,73,75] As they have for the bR and rhodopsin systems, resonance Raman measurements on the P band may provide further insight into this aspect of the problem, and initial experiments in this direction have recently appeared.[81,82] Finally, the possibility of coupling between the initially excited electronic state and a nearby state as discussed above for rhodopsins has also been considered in the context of RCs.[73]

Conclusions

Photochemical hole burning of bacteriorhodopsin and bovine rhodopsin has been performed at wavelengths throughout their lowest energy absorption bands. The observed broad holes were simulated using a wave packet propagation technique and the vibronic and line width parameters determined from previous analyses of resonance Raman intensities. The observation of ~2500-cm^{-1} hole widths with no evidence for narrow zero-phonon features in the two pigments is consistent with very rapid vibronic relaxation on a 10–100-fs time scale in these two systems, even at low temperature. The decrease in the inhomogeneous line width of bacteriorhodopsin and rhodopsin at low temperature from 1100 to 470 cm^{-1} and from 1800 to 700 cm^{-1} fwhm, respectively, can be explained in terms of decreased fluctuations in protein–chromophore interactions. This study illustrates how photochemical holeburning and resonance Raman spectroscopies can be combined to obtain a detailed description of the sources of line broadening in these molecules. This combination of techniques should be generally applicable for investigating other strongy coupled molecular systems.

Note Added in Proof. A direct measurement of the cis–trans isomerization time in rhodopsin was recently reported.[83] Consistent with the picture presented here, these 35-fs pump, 10-fs probe experiments demonstrate that the primary isomerization in vision is essentially complete in only 200 fs.

Acknowledgment. The authors thank Laura Mazzola for help in obtaining the 1.5 K absorption spectrum of isorhodopsin, Dr. Robert Goldstein for experimental assistance in the early stages of this work, and W. Thomas Pollard for insightful discussions. This work was supported by Grants from the National Science Foundation (DMB-8904134, SGB; CHE 86-15093, RAM) and the National Institutes of Health (GM 27738, SGB; EY 02051 and GM 44801, RAM).

Registry No. Retinal, 116-31-4.

(73) Won, Y.; Friesner, R. A. *J. Phys. Chem.* **1988**, *92*, 2214.
(74) Kirmaier, C.; Holten, D. *Photosynth. Res.* **1987**, *13*, 225.
(75) Middendorf, T. R.; Mazzola, L. T.; Gaul, D.; Schenck, C.; Boxer, S. G. *J. Phys. Chem.* **1991**, *95*, 10142.
(76) Mathies, R.; Stryer, L. *Proc. Natl. Acad. Sci. U.S.A.* **1976**, *73*, 2169.
(77) Lockhart, D. J.; Boxer, S. G. *Biochemistry* **1987**, *26*, 664, 2958.
(78) Lockhart, D. J.; Boxer, S. G. *Proc. Natl. Acad. Sci. U.S.A.* **1988**, *85*, 107.
(79) Lösche, M.; Feher, G.; Okamura, M. Y. *Proc. Natl. Acad. Sci. U.S.A.* **1987**, *84*, 7537.
(80) Middendorf, T. R.; Gottfried, D. S.; Lockhart, D. J.; Johnson, D. G.; Wasiliewski, M.; Boxer, S. G., manuscript in preparation.
(81) Donohoe, R. J.; Dyer, R. B.; Swanson, B. I.; Violette, C. A.; Frank, H. A.; Bocian, D. F. *J. Am. Chem. Soc.* **1990**, *112*, 6716.
(82) Shreve, A.; Cherepy, N.; Franzen, S.; Boxer, S. G.; Mathies, R. A. *Proc. Natl. Acad. Sci. U.S.A.*, in press.
(83) Schoenlein, R. W.; Peteanu, L. A.; Mathies, R. A.; Shank, C. V. *Science* **1991**, *254*, 412.